15TH IEA HEAT PUMP CONFERENCE
MAY 26–29, 2026 | HOFBURG
VIENNA 2026
DECARBONISATION THROUGH INNOVATION

Evaluation of the influence of air maldistribution on the refrigerant charge in a finned tube heat exchanger

David Alarcón-Gallén[a], Raffaele Cilento[b], Belén Llopis-Mengual[a], Francesco Pelella[b], Luca Viscito[b], Alfonso William Mauro[b], Emilio Navarro-Peris[a*]

[a]Instituto Universitario de Investigación de Ingeniería Energética (IUIIE), Universitat Politècnica de València (UPV), Camino de Vera s/n, 46022 Valencia, Spain
[b]Department of Industrial Engineering, Università degli Studi di Napoli–Federico II, P.le Tecchio 80, 80125 Naples, Italy

Abstract

Most of the refrigerant fluids with low Global Warming Potential has as a drawback the fact that they are flammable. This fact has made charge minimization and therefore the analysis of the refrigerant charge required in a heat pump a very relevant topic nowadays. Nevertheless, the theoretical estimation of the charge in a heat pump is not a solved problem as it is affected by several factors like the knowledge of internal volumes, the precise determination of the refrigerant flow conditions, the refrigerant-oil solubility or the maldistribution of refrigerant among the different circuits of the system.
In this paper we analyze the influence of air maldistribution in the estimation of the refrigerant charge of an air to water heat pump. This factor usually is not considered in this kind of system but could be important as this maldistribution could be originated by the system design itself but can be introduced also during the operation of the system because of some fouling on it. Findings reveal that air maldistribution could significantly affect refrigerant distribution in finned tube evaporators with several circuits leading to important variations in the refrigerant charge demanded by the heat exchanger. This fact could introduce relevant performance degradation especially in systems without liquid receivers, in which the minimization of charge could be an objective.

Selection and/or peer-review under the responsibility of the organizers of the 15th IEA Heat Pump Conference 2026.

Keywords: air maldistribution; finned-tube heat exchanger; refrigerant charge; heat pump; propane

1. Introduction

The transition to refrigerants with low Global Warming Potential (GWP) is a key strategy for mitigating the climate change impacts of the Heating, Ventilation, Air Conditioning, and Refrigeration (HVAC&R) sectors, driven by international protocols and regulations [1] [2]. However, many of the most viable low-GWP refrigerants, such as R1234yf or propane (R290), are classified as A2L (lower flammability) or A3 (flammable), respectively. This flammability introduces significant safety concerns and regulatory constraints regarding their use in public and residential spaces [3] [4]. As a result, minimizing the total refrigerant charge in heat pump systems has become a critical design and operational objective. Accurate estimation and management of the refrigerant charge are essential not only for safety but also for optimizing system performance, ensuring energy efficiency, and complying with international standards [5].

Despite its importance, the precise estimation of the refrigerant charge required for optimal operation remains a significant challenge. This task is complicated by several factors, including the difficulty in accurately modeling the two-phase (liquid-vapor) distribution within the heat exchangers, which often relies on void fraction correlations that vary in their applicability [6], complex solubility of refrigerant in the compressor lubricating oil [7] or refrigerant maldistribution (two-phase) among the different circuits of an evaporator [8].

While these factors are widely recognized, the capacity of the air-side maldistribution to induce an impact on the refrigerant charge inventory has received comparatively little attention. Air-side maldistribution is common in compact finned-tube heat exchangers, where it can be caused by unit geometry, fan placement, or operational faults such as filter clogging or progressive coil fouling [9]. Most research on this topic has focused on the resulting degradation of performance, namely the reduction in heating/cooling capacity and Coefficient of Performance (COP).

However, a non-uniform airflow profile also forces the parallel refrigerant circuits to operate under different conditions. This effect was highlighted in a numerical and experimental study by Guzzardi et al. [9]. They indicate that this maldistribution could increase the total refrigerant charge required in a chiller by up to 12.7% and decrease system performance by 11%. This occurs because circuits exposed to low airflow may fail to condense fully the refrigerant, while circuits in high-airflow zones become deeply subcooled, thus altering the total liquid refrigerant mass held within the heat exchanger.

This relationship between air distribution and charge inventory has direct and critical implications for the field of Fault Detection and Diagnosis (FDD) [10] [11]. Soft faults, such as refrigerant leakage or heat exchanger fouling, are notoriously difficult to detect as they typically cause gradual performance degradation rather than immediate failure [12]. Air-side fouling itself causes airflow maldistribution, which means that an unidentified, pre-existing maldistribution (either due to design or fouling) could change the system's baseline operating parameters and refrigerant charge requirements. This phenomenon could potentially mask the symptoms of other critical faults, particularly refrigerant leakage. For instance, if a specific maldistribution pattern causes the condenser to retain more liquid refrigerant, the system may tolerate a greater mass of leaked refrigerant before undercharge symptoms or significant performance drops manifest. This could allow a critical fault to go undetected, leading to prolonged inefficient operation or eventual component failure.

The objective of this study is to experimentally evaluate how controlled air-side maldistribution patterns affect the refrigerant distribution and total charge requirements in a multi-circuit finned-tube heat exchanger. To isolate the effect of air-side maldistribution from the known challenge of two-phase refrigerant distribution at the inlet, this work focuses on an air-to-water heat pump operating in cooling mode. In this configuration, the finned-tube heat exchanger functions as the condenser, receiving superheated vapor at its inlet, which is expected to distribute evenly among the parallel circuits under uniform air conditions. By imposing known blocking patterns on the air side, it can be directly characterized if there is refrigerant maldistribution and its impact on the charge inventory as a direct consequence of the non-uniform air velocity. The novelty of this work lies in providing experimental data that quantifies this phenomenon on a condenser, offering a basis for improving the information for developing FDD algorithms to work effectively in case of simultaneous faults of refrigerant leakage with air-side non-uniformity.

2. Methodology

2.1. Experimental setup

The experimental setup consisted of a residential-type air-to-water heat pump (3.5 kW nominal capacity) utilizing R290 (propane) as the working fluid. The unit, equipped with a hermetic rotary compressor, an electronic expansion valve, a finned-tube heat exchanger, and a brazed plate heat exchanger, was tested within a climatic chamber able to maintain steady-state air and water conditions.

The liquid receiver of the unit was removed in such a way that any variation in the system's refrigerant requirement manifests as a directly observable change in the subcooling (SC) at the condenser outlet. The main geometry parameters of this air heat exchanger are described in Table 1.

The unit was comprehensively instrumented for thermodynamic monitoring. Table 2 lists the primary measurement instruments and their total error.

Temperatures were measured using PT100 RTDs (for inlet/outlet air and water temperatures) and Type T thermocouples (for refrigerant inlet/outlet temperatures of every component). Pressure was measured with pressure transducers at the compressor suction and discharge. Refrigerant and water mass flow rates were measured using Coriolis mass flow meters. The electrical power consumption was monitored independently using a wattmeter.

Since this study focuses on the 8-circuit finned-tube heat exchanger, a Type T thermocouple was installed at the outlet of each of the eight circuits (in cooling mode). This instrumentation allows for the direct evaluation of the subcooling for each individual circuit, which serves as the primary indicator of possible refrigerant maldistribution.

Table 1. Geometry data of the finned tube heat exchanger

Pipes spacing [mm]	25
Pipes per row	32
Rows	3
Fin spacing [mm]	1.8
Fin thickness [mm]	0.1
Number of Circuits	8
External pipe diameter [mm]	7
Estimated Volume [L]	2.33

Table 2. Measurement instruments used in the experimental campaign and their range and total error.

Measurement	Instrument	Range	Total error
Refrigerant temperature	Thermocouple type T	-270-400ºC	±0.8 (ºC)
Water and air temperature	Thermorresistance PT-100	-220-850ºC	±0.07 (ºC)
Suction and discharge pressure	Pressure transducer Rosemount 3051	0-15 bar/10-45 bar	±0.06 (bar)
Refrigerant mass flow rate	Coriolis flowmeter Micro Motion CMFS015M	0-5600 kg/h	±0.13 (kg/h)
Water mass flow rate	Coriolis flowmeter Mass 2100	0-245 kg/h	±4.48 (kg/h)
Total power input	Power meter A2000 Gossen Metrawatt	0-2.5 kW (configured)	±0.0144 (kW)

2.2. Test campaign

To evaluate the influence of maldistribution across different refrigerant inventories, the system was tested at two distinct R290 charge levels: 480 g and 580 g. The airflow across the heat exchanger was intentionally manipulated to simulate non-uniform distribution. These faulty-state results were compared against a baseline test conducted under normal, non-manipulated airflow conditions (called "No Blockage").

The experimental campaign was conducted with the heat pump operating exclusively in cooling mode. This mode was selected because the finned-tube heat exchanger functions as the condenser, which retains a significantly larger portion of the system's refrigerant charge compared to the evaporator, as well as because the distribution of refrigerant monophasic flow at the inlet of the heat exchanger is less sensible to present an initial maldistribution. These characteristics make easier to check the effects of any refrigerant maldistribution induced by an air flow maldistribution, thereby facilitating a more robust measurement and analysis. The two steady-state operating conditions used for the tests are summarized in Table 3.

Table 3. Experimental operating conditions (in cooling mode).

Ambient Air Temperature [°C]	Water Return - Production Temperature [°C]	Compressor speed [rps]
30	23 - 18	60
35	12 - 7	45

To simulate non-uniform airflow, controlled blockage patterns were applied to the air-inlet face of the heat exchanger using cardboard panels. To ensure stable and repeatable placement, the panels were attached to the exchanger's front surface using custom 3D-printed couplings equipped with hook-and-loop fasteners (Fig. 1).

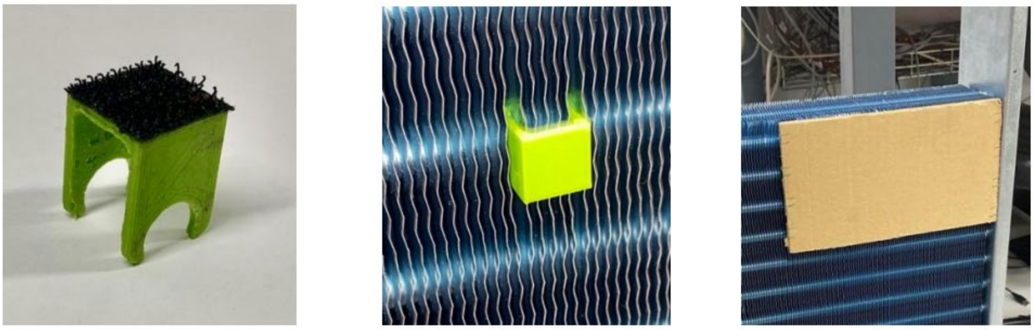

Figure 1. 3D clip with Velcro (left), clip on the heat exchanger (center), cardboard on the heat exchanger (right).

The frontal area of the heat exchanger was conceptually divided into an 8x4 matrix (8 horizontal sections corresponding to the refrigerant circuits and 4 vertical sections) to guide the application of these patterns, as shown in Fig. 2. A total of eight distinct blockage patterns were selected for the experimental campaign, which are also illustrated in Fig. 2. These patterns were divided into two main sets. The first set consisted of five single-circuit blockages (12.5% blockage each), targeting individual circuits at specific locations: one at the top (Circuit A), two in the center (Circuits C and D), and two near the bottom (Circuits G and H). The second set comprised three multi-circuit patterns representing more severe and widespread blockage: "Center" (37.5%), "4 circuits" (50%), and "All edges" (62.5%).

Name	Cells Blocked	Image	Name	Cells Blocked	Image
A circuit	4 (12,5%)		H circuit	4 (12,5%)	
C circuit	4 (12,5%)		All edges	20 (62,5%)	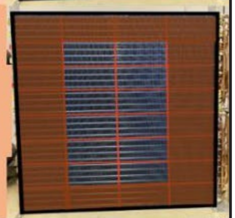
D circuit	4 (12,5%)	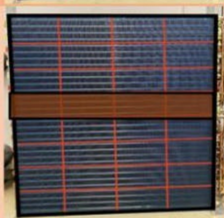	4 circuits	16 (50%)	
G circuit	4 (12,5%)	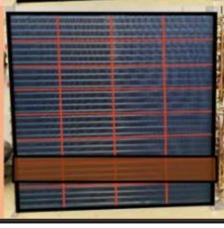	Center	12 (37,5%)	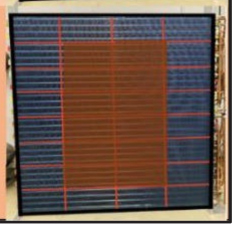

Figure 2. Blockage patterns imposed experimentally to simulate air maldistribution.

2.3. Heat pump model

This heat pump has been modeled with the commercial software IMST-ART [13]. The model includes detailed calculations of all main components: heat exchangers, compressor, expansion device, piping, and other auxiliary parts. Fluid properties are obtained from REFPROP [14].

The heat exchanger submodels use a one-dimensional discretization that accounts for heat transfer and pressure drop. The refrigerant heat transfer coefficient is calculated using correlations for evaporation, for condensation, for single-phase flow, and for the air side [15] [16][17] [18]. Frictional pressure losses in round tubes are estimated with correlations [19] [20]. The finite volume method and the semi-explicit method for the wall-temperature-linked equation are used to solve the heat exchanger discretization [13].

In the finned-tube heat exchanger model, it is also possible to impose a non-uniform air flow profile. This option makes it feasible to include the blockage pattern applied during the experiments in the model. By doing so, the effect of air maldistribution is considered directly in the heat exchanger calculations.

The compressor submodel includes equations for mass flow rate, power input, and heat losses. These relations are derived from catalog data that provide refrigerant mass flow rate and electrical power input at different compressor speeds. For the refrigerant charge calculation, the void fraction correlation is applied [21]. The amount of refrigerant dissolved in the oil is estimated from oil solubility curves at discharge conditions.

The model has been applied in numerous studies and validated through experimental tests, with maximum relative errors generally within 5–10%, as reported, for example, in [22], [23] and [24]. Further details on the modeling and numerical procedures in IMST-ART can be found in [25] and [26].

With all these elements, the model can provide heat pump operating conditions when air data, water data, compressor speed, and the charge or subcooling level are given. Thus, it has been used to estimate the refrigerant charge required by the system based on the external (secondary fluids) and control conditions. By utilizing the measured subcooling values, the charge requirements under varying levels of air maldistribution can be compared.

3. Results and Discussion

3.1. Experimental results

Fig. 3 and 4 show the measured subcooling at each circuit with the 8 blockage patterns imposed and at the different test conditions. Test conditions are expressed using the code “A_W_@_”, which indicates the sink and source temperatures in ºC: “A” (Air inlet temperature), “W” (Water outlet temperature), while what is to the right of “@” represents the compressor speed in rps. The other part of this code shows the refrigerant charged into the unit.

Under baseline "No Blockage" conditions, the subcooling for each of the eight circuits (A-H) shows a deviation which is not higher than ±0.5 K. However, as shown in Fig. 3 (A35W7@45 - 480g), when a specific single-circuit blockage is applied (e.g., "A Circuit" or "C Circuit"), the subcooling of that targeted circuit experiences a pronounced decrease relative to the unblocked circuits. This phenomenon is attributed to the reduced heat transfer in the blocked region, which increases the two-phase region of the heat exchanger, reducing the available area to subcool the refrigerant.

This behavior is consistently observed across different operating conditions. Fig.4 (A30W18@60 - 480g) shows that the system operates with a higher overall degree of subcooling at this test point. This higher baseline condition serves to magnify the subcooling deviation when a pattern is applied, making the impact of the maldistribution even more apparent. In both test conditions, while the specific subcooling values change, the trend remains the same: regions with restricted airflow are unable to achieve the same level of subcooling as the unblocked regions, confirming a direct link between airflow non-uniformity and refrigerant maldistribution at the condenser outlet.

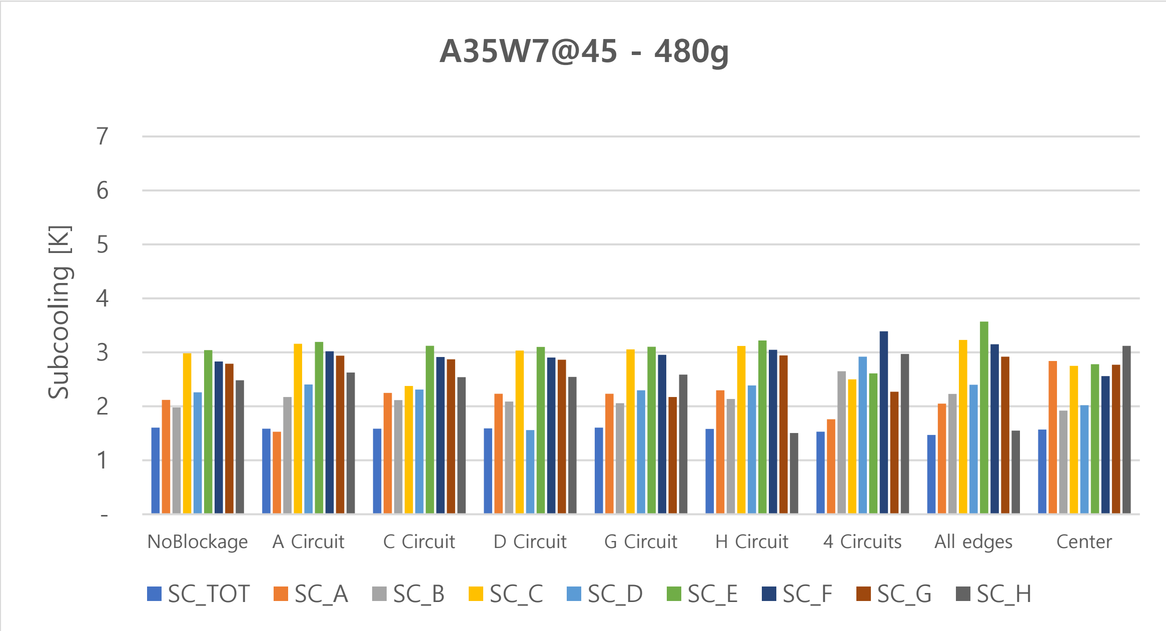

Figure 3. Subcooling (SC) of each circuit with the eight blockage patterns in A35W7@45 conditions and 480g of refrigerant charge.

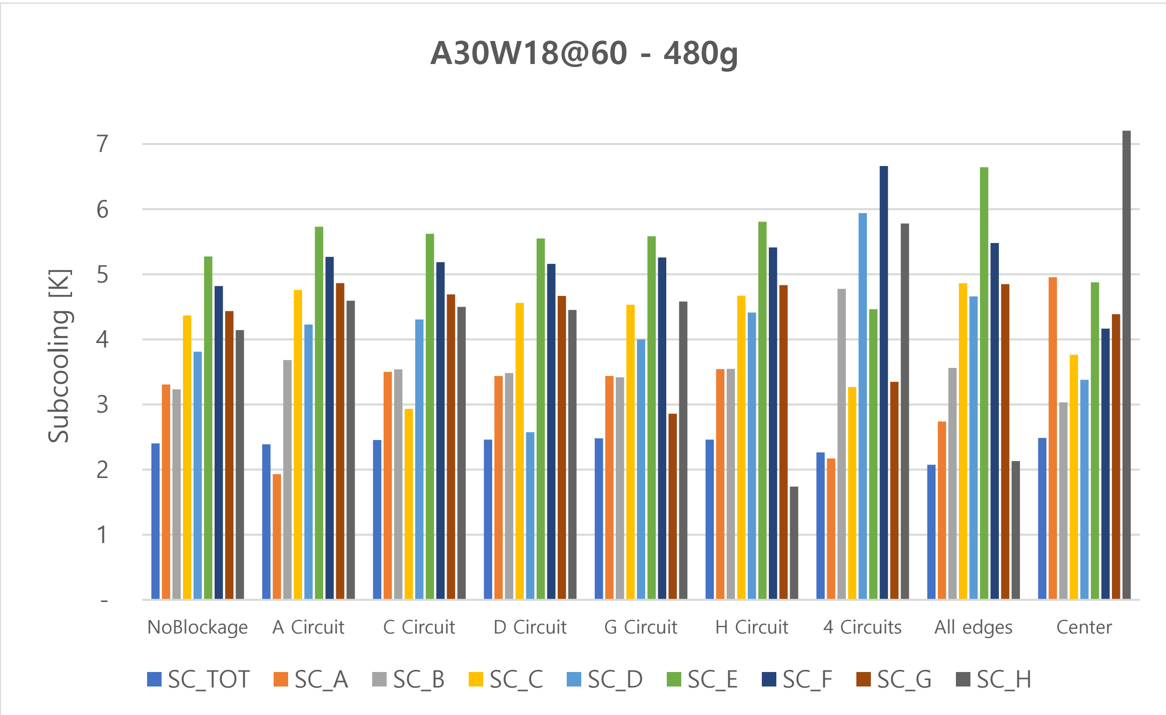

Figure 4. Subcooling (SC) of each circuit with the eight blockage patterns in A30W18@60 conditions and 480g of refrigerant charge.

Fig.5 presents a summary of the four cases studied, showing the subcooling variations in each circuit relative to the values measured in the no-blockage case. The figure shows that some circuits reach differences of up to 6 K, which reflects the change in how the refrigerant is distributed inside the condenser.

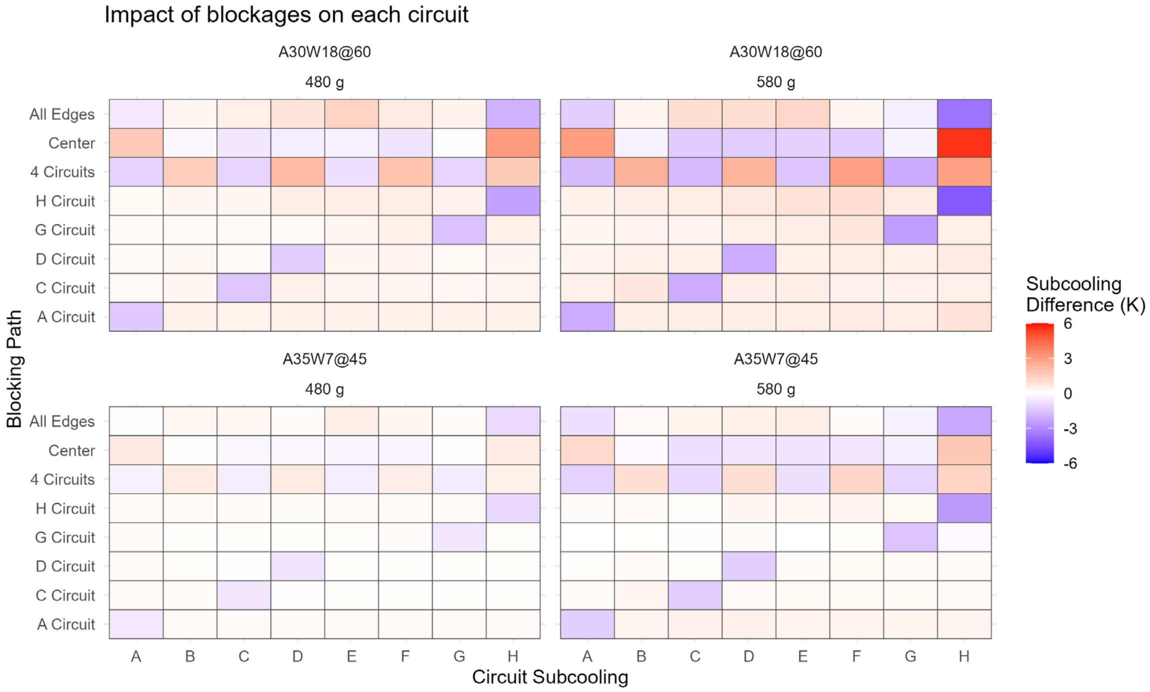

Figure 5. Change in circuit subcooling for each blockage pattern relative to the No Blockage case

3.2. Effect of air maldistribution on the charge requirements

As shown in the previous section, the subcooling results obtained for each circuit under the different blockage patterns suggest that air maldistribution leads to an uneven refrigerant distribution in the condenser. Some circuits hold more refrigerant than others. To examine this effect, the measured subcooling of each circuit was imposed in the heat pump model. This makes it possible to estimate the share of refrigerant charge held in each circuit. Fig. 6 shows the results for the A30W18 test at 60 rps, where the total charge was set to 580 g.

First, even in the "No blockage" case, the distribution is not perfectly uniform. A fully uniform distribution would correspond to 12.5% charge in each circuit. The model results show that the distribution is reasonably close to this level, although the middle and lower circuits store slightly more charge than the upper ones.

When individual circuits are covered, the amount of refrigerant held in those circuits decreases, and part of the charge moves to the remaining circuits. This behaviour appears clearly in the cases where circuits A, C, D, G, or H are covered. For blockage patterns that impose stronger air maldistribution, such as the "4 circuits" case, the refrigerant again shifts from the covered circuits to the open ones, which hold a larger share of the total charge.

The "all edges" pattern leads to less refrigerant in the upper and lower circuits, since these are fully covered. The middle circuits, although slightly affected by the edges, hold more charge because they retain more free area for heat exchange. In contrast, the "center" pattern shows the opposite trend: the central circuits retain less refrigerant due to the blockage, while the upper and lower circuits concentrate most of the charge. In this case, the lower circuit holds 15.1% of the condenser charge.

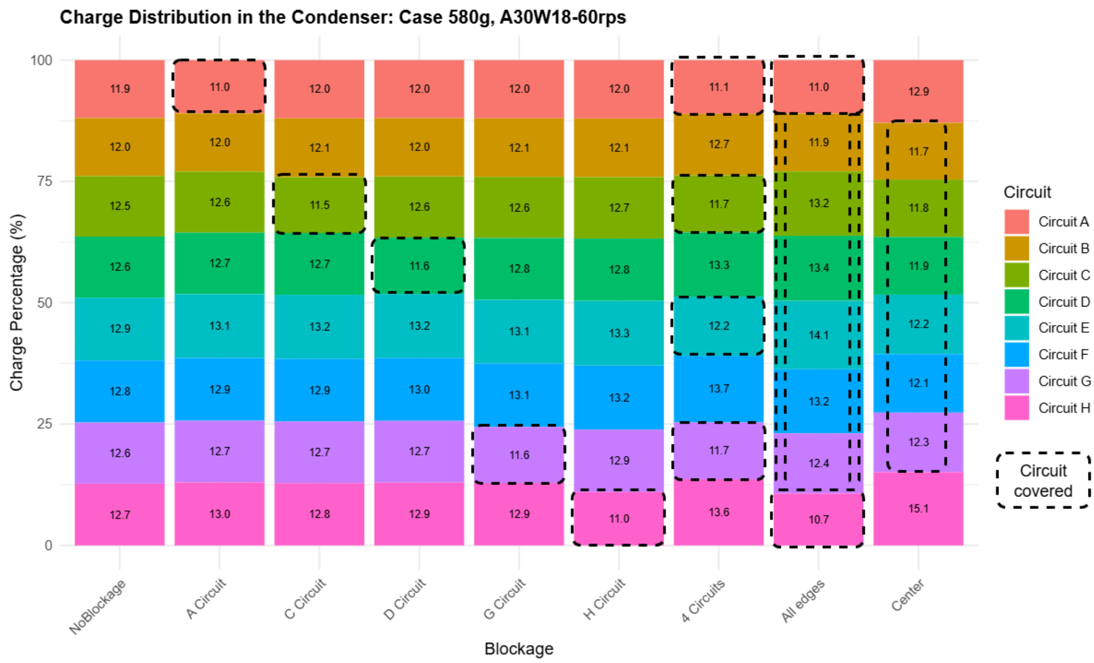

Figure 6. Estimated refrigerant charge share in each condenser circuit with every blockage pattern imposed for the A30W18 test at 60 rps.

From these results, it becomes clear that the refrigerant is unevenly distributed among the condenser circuits due to the air maldistribution produced by each blockage pattern. This uneven refrigerant distribution can have a strong effect on the charge required by the system. As shown earlier, when air flows more easily through a given circuit (that is, when it is free of blockage in this study), the subcooling is higher and more refrigerant accumulates in that part of the condenser. In other words, under air maldistribution, the condenser needs less refrigerant to reach the observed subcooling levels, which means that the system is effectively overcharged for that condition. This explains the high subcooling values measured in the circuits that are free of blockage.

The model was used to estimate how much excess refrigerant the system holds under the different blockage patterns. The measured subcooling of each circuit was used as input, for both tested conditions: A35W7 at 45 rps and A30W18 at 60 rps. Two imposed charges, 480 g and 580 g, were also examined, since the measured subcooling changes with the total charge, as shown earlier. Fig. 7(a) shows how the calculated charge requirements vary under each blockage pattern.

The results show that when only a single circuit is covered, the change in charge requirement is small, and the system needs nearly the same amount of refrigerant to operate. However, for more severe cases where several circuits are affected, the situation changes. For example, under the “4 circuits” or “center” patterns, the system operates with roughly 8% excess refrigerant. Under the “all edges” pattern, the excess ranges from about 30% to 70%, depending on the condition. This means that, in such cases, if a refrigerant leak occurred, it would take much longer to detect it. The reason is that with these fouling-related patterns that reduce air uniformity, the system naturally requires less refrigerant to operate.

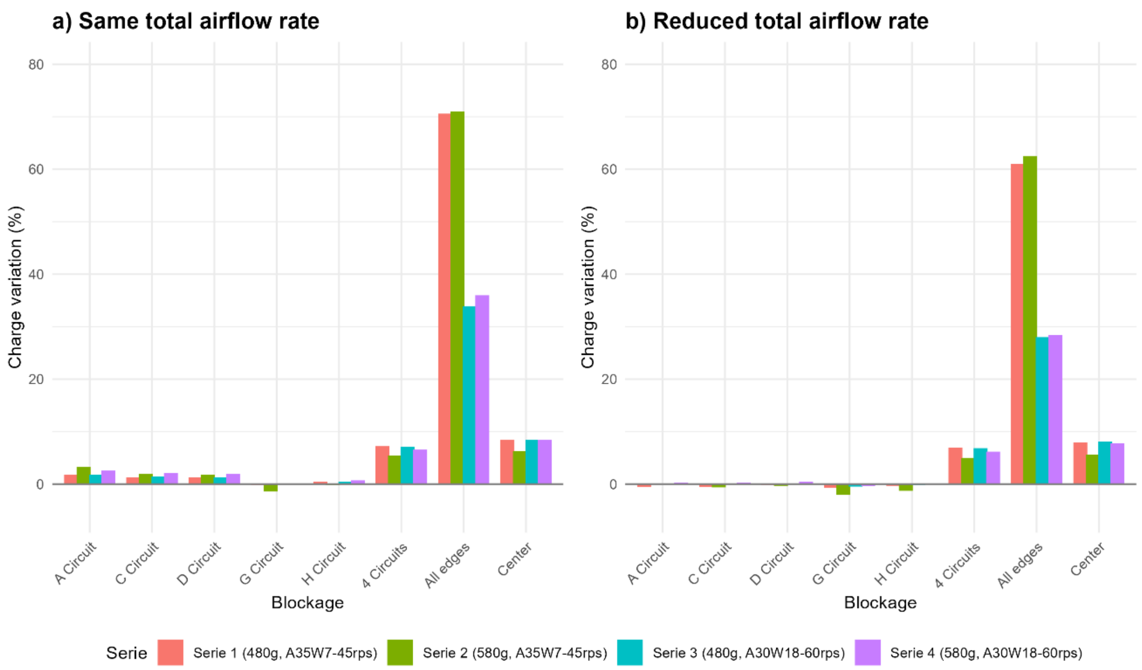

Figure 7. Charge requirements estimated from measured circuit subcooling under different air blockage patterns. a) With the same total airflow rate and b) reducing the total airflow rate through the heat exchanger.

Fig. 7(b) shows the same analysis but with an additional reduction of the total air flow rate imposed in the model. This is relevant because, in practice, air maldistribution produced by dirt or debris usually introduces an added pressure drop on the air side, which reduces the total flow rate. The cardboard plates used experimentally also introduced this extra pressure drop. The results, however, indicate that the reduction in total air flow does not significantly change the charge requirements seen in Fig. 7(a). This confirms that the main driver of the change in charge requirement is the air maldistribution pattern itself, which causes an uneven refrigerant distribution, rather than the reduction in total airflow.

It should be noted that the charge variations reported in Fig. 7 are derived from model calculations and not from experimental operation of the unit at undercharged conditions. The results indicate that the dominant factor affecting the required charge is the severity of air maldistribution, which promotes an uneven refrigerant distribution among circuits. By contrast, a uniform reduction in total air flow rate, such as that caused by fouling, has a comparatively small impact on the overall charge requirement.

4. Conclusions

The results show that the way air is distributed over the condenser surface has a direct effect on how the refrigerant is distributed among the circuits. Even partial and localized blockages cause noticeable changes in the subcooling measured in each circuit, which confirms that small differences in air flow already modify the thermodynamic state of the refrigerant. When the blockage patterns affect several areas of the surface, these differences become stronger, leading some circuits to hold more refrigerant. This means that the system no longer operates under the expected conditions, even if the total air flow rate remains similar, because the key factor is how the air is distributed over the heat exchanger surface.

The model results confirm that this behavior has a clear effect on the amount of refrigerant needed for the unit to reach the measured subcooling values. In the cases with severe blockage, the unit can operate with 30–70% less refrigerant without showing obvious signs of malfunction, which makes leak detection more difficult during real operation. This is especially relevant for units without a liquid receiver, where the charge strongly influences performance. Therefore, non-uniform air distribution not only reduces capacity and COP but also changes the reference conditions used to identify other faults. This effect should be considered when designing diagnostic methods, since it can hide or delay the detection of refrigerant leaks or fouling on the air side.
This air effect could have similar consequences on the refrigerant charge of the evaporator but in this case we can have also the effect of non-uniform frost formation.

Acknowledgements

The authors gratefully acknowledge the European Innovation Council Pathfinder Program Grant BEYOND, with project ID: 101162436 – Funded by the European Union under Horizon Europe.

References

[1] European Parliament, "Regulation (EU) 2024/573 of the European Parliament and of the Council of 7 February 2024 on fluorinated greenhouse gases, amending Directive (EU) 2019/1937 and repealing Regulation (EU) No 517/2014," 2024. [Online]. Available: https://eur-lex.europa.eu/eli/reg/2024/573/oj

[2] E. A. Heath, "Amendment to the Montreal Protocol on Substances that Deplete the Ozone Layer (Kigali Amendment)," *International Legal Materials*, vol. 56, no. 1, pp. 193–205, 2017, doi: 10.1017/ilm.2016.2.

[3] "EN 378: 2016. Refrigeration systems and heat pumps – environmental requirements," 2016.

[4] ASHRAE, "ANSI/ASHRAE Standard 15-2022, Safety Standard for Refrigeration Systems," 2022.

[5] J. M. Corberán, I. Martínez-Galván, S. Martínez-Ballester, J. Gonzálvez-Maciá, and R. Royo-Pastor, "Influence of the source and sink temperatures on the optimal refrigerant charge of a water-to-water heat pump," *International Journal of Refrigeration*, vol. 34, no. 4, pp. 881–892, 2011, doi: 10.1016/j.ijrefrig.2011.01.009.

[6] T. M. Harms, E. A. Groll, and J. E. Braun, "Accurate charge inventory modeling for unitary air conditioners," *HVAC and R Research*, vol. 9, no. 1, pp. 55–78, 2003, doi: 10.1080/10789669.2003.10391056.

[7] L. Sánchez-Moreno-Giner, T. Methler, F. Barceló-Ruescas, and J. Gonzálvez-Maciá, "Refrigerant charge distribution in brine-to-water heat pump using R290 as refrigerant," *International Journal of Refrigeration*, vol. 145, no. October 2022, pp. 158–167, 2023, doi: 10.1016/j.ijrefrig.2022.10.013.

[8] L. Pu, L. Nian, D. Zhang, T. Gu, M. Liu, Y. Zhou, F. Yuan, and W. Chen, "Study of refrigerant mal-distribution and optimization in distributor for air conditioner," *Sustainable Energy Technologies and Assessments*, vol. 46, no. November 2020, p. 101261, 2021, doi: 10.1016/j.seta.2021.101261.

[9] C. Guzzardi, M. Azzolin, S. Lazzarato, and D. Del Col, "Refrigerant mass distribution in an invertible air-to-water heat pump: effect of the airflow velocity," *International Journal of Refrigeration*, vol. 138, no. March, pp. 180–196, 2022, doi: 10.1016/j.ijrefrig.2022.03.006.

[10] B. Llopis-Mengual and E. Navarro-Peris, "Effects of simultaneous soft faults in a reversible and variable-speed air-to-water heat pump," *Appl Therm Eng*, vol. 254, no. October, Jul. 2024, doi: 10.1016/j.applthermaleng.2024.123883.

[11] F. Pelella, L. Viscito, and A. William Mauro, "Combined effects of refrigerant leakages and fouling on air-source heat pump performances in cooling mode," *Appl Therm Eng*, vol. 204, no. December 2021, p. 117965, 2021, doi: 10.1016/j.applthermaleng.2021.117965.

[12] I. Bellanco, E. Fuentes, M. Vallès, and J. Salom, "A review of the fault behavior of heat pumps and measurements, detection and diagnosis methods including virtual sensors," *Journal of Building Engineering*, vol. 39, no. January, p. 102254, 2021, doi: 10.1016/j.jobe.2021.102254.

[13] J. M. Corberán, P. Fernández de Córdoba, J. Gonzálvez, and F. Alias, "Semiexplicit method for wall temperature linked equations (sewtle): a general finite-volume technique for the calculation of complex heat exchangers," *Numerical Heat Transfer, Part B: Fundamentals*, vol. 40, no. 1, pp. 37–59, Jul. 2001, doi: 10.1080/104077901300233596.

[14] E. W. Lemmon, I. H. Bell, M. L. Huber, and M. O. McLinden, "NIST Standard Reference Database 23: Reference Fluid Thermodynamic and Transport Properties-REFPROP, Version 10.0, National Institute of Standards and Technology." 2018. doi: https://doi.org/10.18434/T4/1502528.

[15] VDI-Verlag GmbH, Ed., *VDI Heat Atlas*. Düsseldorf, 1993.

[16] A. Cavallini, G. Censi, D. Del Col, L. Doretti, G. A. Longo, and L. Rossetto, "In-tube condensation of halogenated refrigerants," in *ASHRAE Transactions*, Atlanta: ASHRAE, 2002. [Online]. Available: http://dx.doi.org/10.1016/j.jaci.2012.05.050

[17] V. Gnielinski, "New equations for heat and mass transfer in turbulent pipe and channel flow," *International Chemical Engineering*, vol. 16, pp. 359–368, 1976.

[18] C. C. Wang, Y. M. Hwang, and Y. T. Lin, "Empirical correlations for heat transfer and flow friction characteristics of herringbone wavy fin-and-tube heat exchangers," *International Journal of Refrigeration*, vol. 25, no. 5, pp. 673–680, 2002, doi: 10.1016/S0140-7007(01)00049-4.

[19] L. Friedel, "New friction pressure drop correlations for upward, horizontal, and downward two-phase pipe flow," in *HTFS Symposium*, Oxford, 1979.

[20] S. W. Churchill, "Friction Factor Equation Spans All Fluid Flow Regimes," *Chemical Engineering*, vol. 84, pp. 91–92, 1977.
[21] D. Steiner and J. Taborek, "Flow Boiling Heat Transfer in Vertical Tubes Correlated by an Asymptotic Model," *Heat Transfer Engineering*, vol. 13, no. 2, pp. 43–69, Jan. 1992, doi: 10.1080/01457639208939774.
[22] J. R. García-Cascales, F. Vera-García, J. M. Corberán-Salvador, and J. Gonzálvez-Maciá, "Assessment of boiling and condensation heat transfer correlations in the modelling of plate heat exchangers," *International Journal of Refrigeration*, vol. 30, no. 6, pp. 1029–1041, Sep. 2007, doi: 10.1016/j.ijrefrig.2007.01.004.
[23] M. Pitarch, E. Hervas-Blasco, E. Navarro-Peris, and J. M. Corberán, "Exergy analysis on a heat pump working between a heat sink and a heat source of finite heat capacity rate," *International Journal of Refrigeration*, vol. 99, pp. 337–350, Mar. 2019, doi: 10.1016/j.ijrefrig.2018.11.044.
[24] B. Llopis-Mengual, D. P. Yuill, and E. Navarro-Peris, "Fault detection and diagnosis algorithm for multiple simultaneous faults in residential air-conditioning systems: Development, validation study and critical analysis," *Appl Therm Eng*, p. 125975, Feb. 2025, doi: 10.1016/j.applthermaleng.2025.125975.
[25] A. H. Hassan, J. M. Corberán, M. Ramirez, F. Trebilcock-Kelly, and J. Payá, "A high-temperature heat pump for compressed heat energy storage applications: Design, modeling, and performance," *Energy Reports*, vol. 8, pp. 10833–10848, 2022, doi: 10.1016/j.egyr.2022.08.201.
[26] B. Llopis-Mengual and E. Navarro-Peris, "Selection of relevant features to detect and diagnose single and multiple simultaneous soft faults in air-source heat pumps," *Appl Therm Eng*, vol. 238, no. April 2023, p. 121922, Feb. 2024, doi: 10.1016/j.applthermaleng.2023.121922.